Superfluidity in polariton condensates

2010 J. Phys.: Conf. Ser. 210 012060

(http://iopscience.iop.org/1742-6596/210/1/012060)

Journal of Physics: Conference Series **210** (2010) 012060 doi:10.1088/1742-6596/210/1/012060

Superfluidity in polariton condensates

A Amo[1,2], J Lefrère[1], C Adrados[1], E Giacobino[1] and A Bramati[1]

[1] Laboratoire Kastler Brossel, UPMC, ENS and CNRS, 75005 Paris, France

D Sanvitto[2], F P Laussy[2], D. Ballarini[2], E del Valle[2], M D Martín[2], C Tejedor[2] and L Viña[2]

[2] SEMICUAM, Universidad Autónoma de Madrid, 28049 Madrid, Spain

S Pigeon and C Ciuti

Laboratoire Matériaux et Phénomènes Quantiques, UMR 7162, Université Paris Diderot-Paris 7 and CNRS, 75013 Paris, France

I Carusotto

BEC-CNR-INFM and Dip. di Fisica, Universitá di Trento, I-38050 Povo, Italy

R Houdré

Institut de Photonique et d'Electronique Quantique, Ecole Polytechnique Fédérale de Lausanne, Station 3, CH-1015 Lausanne, Switzerland.

A Lemaître and J Bloch

Laboratoire de Photonique et de Nanostructures, CNRS, Route de Nozay, 91460 Marcoussis, France

D N Krizhanovskii and M S Skolnick

Department of Physics & Astronomy, University of Sheffield, S3 7RH, Sheffield, United Kingdom

E-mail: alberto.amo@spectro.jussieu.fr

Abstract. Exciton-polaritons, two-dimensional composite bosons arising from the quantum mixture of excitons and photons, can manifest many-body quantum effects at liquid He temperatures (4 K). Interestingly, polaritons are predicted to behave as particular quantum fluids due to their out of equilibrium character, arising from their reduced lifetime (shorter than their thermalization time). Here we report the observation of superfluid motion of polaritons in semiconductor microcavities both under cw and pulsed excitation. Among other signatures, superfluidity is manifested via the absence of scattering of the polariton condensates when encountering a localized defect in their flow path.

1. Introduction

Superfluidity is one of the most conspicuous quantum phenomena due to the counterintuitive effects to which it gives rise in the macroscopic scale. First observed in 1938 via the abrupt drop of the viscosity of liquid ^{4}He below the lambda point [1,2], a wide variety of observable facts in different systems can be explained within the framework of superfluidity [3,4]. Some of them are the so called Hess-Fairbank effect (the absence of rotation of a superfluid when the angular velocity of its container is below some critical value) observed both in ^{4}He and in condensates of alkali atoms [5,6], or the appearance of metastable superflows [7-9] quite intimately related to quantized vortex formation [10,11].

However, the most popular image of superfluidity is that of the flow without friction, which corresponds to the above mentioned reports of 1938 on ^{4}He, and it is directly accounted for by the theory of Landau [12]. Within this theory, due to the linearized spectrum of excitations around the ground state of a Bose-Einstein condensate subject to particle-particle interactions, there exists a critical velocity for an object traversing the fluid, below which no excitation of the fluid is possible, resulting in an unperturbed flow. Above such velocity, the travelling object is able to scatter with the fluid giving rise to density perturbations. The critical velocity is given by the slope of the spectrum of excitations of the condensate, and is known as the sound speed of the fluid, c_s. Such condition for the definition of superfluid behaviour is known as the Landau criterion. In Superfluidity according to this criterion has been observed by sending ions and atoms at a controlled speed through bulk ^{4}He [13,14], ^{4}He droplets [15] and atomic BECs [16] and, in the latter case, also by the use of bigger potential barriers moving through the whole condensate [17].

In this work we will present a detailed account of superfluid behaviour in the sense of flow without friction, in a bosonic system out of equilibrium: polaritons in semiconductor microcavities. First experimental evidences of polariton superfluidity were provided in [18], in a configuration based on the optical parametric oscillator, and later in a cw experiment [19]. Under cw conditions we will show that when the polariton gas flows below the sound velocity, scattering with defects present in the sample is inhibited, while above it, density modulations in the form of Čerenkov-like wave-fronts are excited, in agreement with the Landau criterion of superfluidity. In a time resolved configuration, we will show that polariton droplets with a well defined momentum can be created, evidencing no scattering when traversing defects present in their flow path, in agreement with the notion of flow without friction in superfluids.

2. Semiconductor microcavities

Semiconductor microcavities are two-dimensional heterostructures in which one or several quantum wells are embedded in a cavity conformed by two high-reflectivity Bragg mirrors, in which exciton and photon modes are in resonance. Under strong coupling conditions, the eigenstates of such a system are polaritons, composite bosons with a very low mass and short lifetime due to their photonic component, which leads to their annihilation by emission of a photon within a few picoseconds. The emitted photons carry much of the information of the polariton state inside the cavity, rendering accessible the study of polariton gases through photoluminescence studies. Additionally, their excitonic component provides with strong inter-particle interactions which are essential for the apparition of superfluidity in bosonic gases.

Their very light mass, on the order of 10^{-5} times the free electron mass, has enabled the observation at liquid He temperatures of phenomena related to the appearance of macroscopic coherence, like Bose-Einstein condensation [20,21], long-range order [22] or, recently, the spontaneous formation of vortices [23] and persistent currents [24].

3. Polariton superflow under cw excitation

In this section we will present results on the polariton fluid characteristics under cw excitation. In order to probe the superfluidity of polaritons we study the perturbation that is produced in a resonantly created moving polariton fluid, excited with a cw laser, when a static microcavity defect is present in

its flow path [19], as proposed in [25,26]. As we will see, the perturbation created by the defect on the flow, which is evidenced through both the real space density profile and the momentum distribution of the emitted polaritons, provides relevant information on the structure of the spectrum of excitations of the condensate. This fact enables us to directly apply the Landau criterion of superfluidity. Our results are well reproduced by simulations based on the Gross-Pitaevskii equation.

In these experiments we use an InGaAs/GaAs based sample with a 2 λ cavity, and one 80 Å quantum well placed at each of the three antinodes of confined optical field, with a Rabi splitting of 5.1 meV. All experiments are performed at 5 K, with a circularly polarized excitation beam from a frequency stabilized, single-mode continuous wave Titanium:Sapphire laser. The laser field, quasi-resonant with the lower polariton branch at approximately *zero* exciton-cavity detuning, continuously replenishes the escaping polaritons in the fluid. The beam is focused onto the sample in a spot of ~100 µm in diameter, with angles of incidence between 3.4º and 4.0° [figure 1 (a)]. Images of the surface of the sample (near field emission) and of the far field in transmission configuration are simultaneously recorded on two different high resolution CCD cameras.

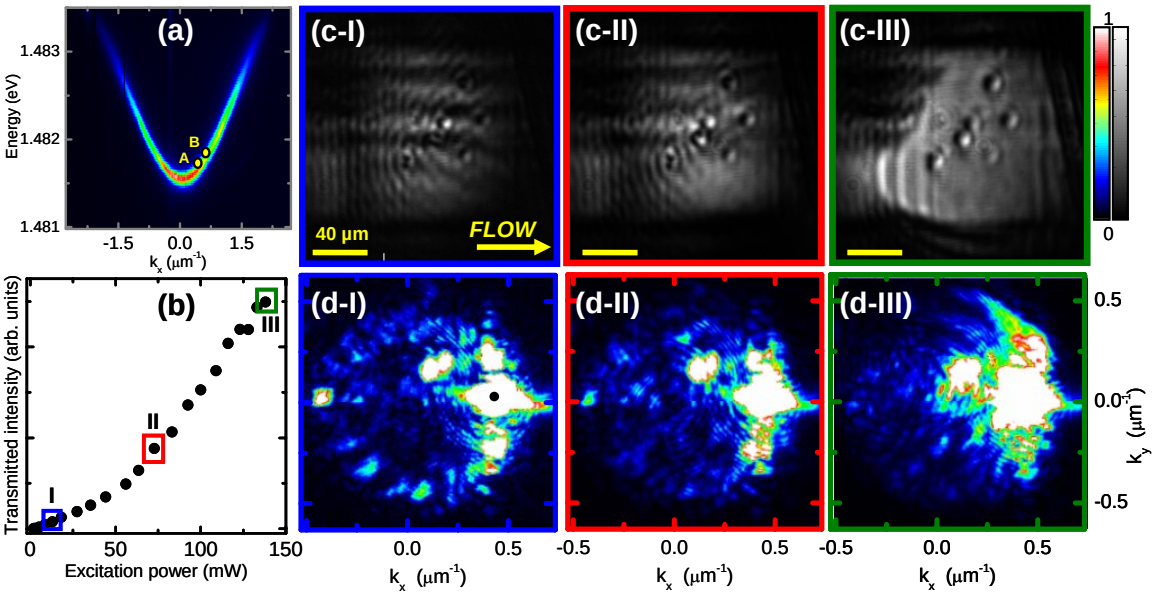

Figure 1. (a) Lower polariton branch dispersion of the InGaAs microcavity at low excitation density. A and B indicate the energy and momentum of the excitation beam corresponding to the conditions of figure 1 and 2 respectively. (b) Transmitted intensity as a function of excitation density for point A in (a): angle of incidence 3.4º, i.e., k = 0.436 µm-1. (c) Real and (d) momentum space images of the transmitted luminescence for the excitation powers indicated in (b). The momentum space images have been normalized to the total transmitted intensity to put in evidence the collapse of the Rayleigh ring.

Figure 1 shows the real (c) and momentum (d) space images of a polariton fluid at different excitation powers (b), for a Gaussian excitation spot on top of 6 point like defects, naturally present in the sample. The pump angle of incidence is 3.4º, corresponding to an in-plane momentum of k_p = 0.436 µm^{-1}. The energy of the laser is slightly blue detuned (~0.08 meV) with respect to the lower polariton branch at the same *k* in the low density linear regime.

At low excitation power, polariton-polariton interactions are negligible, the spectrum of excitations of the system presents a parabolic energy-momentum dependence, and Bogoliubov modes reduce to single particle excitations [26]. In this case, the initially uniform polariton fluid created by the pump is strongly perturbed by the potential: a series of curved wave-fronts are formed around each defect and propagate away from it [figure 1 (c-I)]. These wave-fronts are the real space manifestation of the

Rayleigh scattering ring that is observed in the far-field images [figure 1 (d-I)], and result from the interference of incident and scattered polaritons. As the incident laser is close to resonance with the linear regime polariton branch, the wave-fronts are approximately parabolic [26].

When the polariton density is increased while keeping the same excitation angle, the onset of polariton-polariton interactions is manifested by a non-linear increase of the transmitted intensity [figure 1 (b) around point II]. These interactions modify the dispersion of the elementary excitation giving rise to a dispersion which is predicted to become linear with a discontinuity of its slope in the vicinity of the pump wave vector k_p [26]. In these circumstances the spectrum of excitations can be well described within the Landau model and the fluid can be assigned a sound velocity, given by $c_s = \sqrt{\hbar g |\psi_c|^2 / m}$, where $|\psi_c|^2$ is the polariton density, g is the polariton-polariton interaction strength, and m is their mass. In the conditions of figure 1, the momentum, oscillation frequency (given by the energy of the pump) and density of the injected polaritons is such that $v_p < c_s$, and the Landau criterion for superfluidity is fulfilled. In such a case, scattering from the defects is inhibited, and the polariton fluid is able to flow without friction as no states are any longer available for scattering at the frequency of the driving polariton field. This regime can be identified in figure 1 (c-III), where the polariton fluid neatly passes around the six defects present in its flow path, while a collapse of the Rayleigh ring in the far field is observed (d-III) evidencing the absence of states to which scattering can take place.

If we increase the velocity of the flow, we can gain access to a different quantum fluid regime, namely that in which $v_p > c_s$. According to the Landau model, in this *supersonic* case the condition for superfluidity is not fulfilled, and a defect present in the flow path will generate Čerenkov-like density waves observable in real space, together with a strong modification of the far field emission [27].

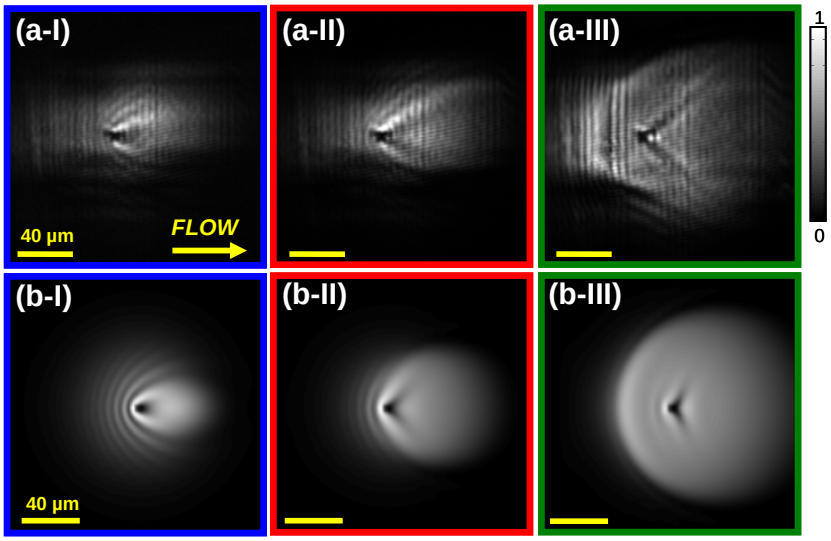

Figure 2. (a) Experimental real space images for a pump momentum $k_p = 0.572$ µm^{-1} (corresponding angle of incidence of 4.4º), for pump powers of 1.83 mW (I), 12.9 mW (II) and 138 mW (III). (b) Simulated images based on the solution of a Gross-Pitaevskii equation with pumping and decay under conditions similar to those of (a).

Figure 2 (a) shows real space images of a polariton fluid in the presence of a single defect for a pump momentum of $k_p = 0.572$ µm^{-1}, corresponding to point B in figure 1 (a), larger than that of figure 1 (b-d). Again, at low excitation density [2 (a-I)] the interference of scattered polaritons and those transmitted with the momentum of the pump gives rise to quasi-parabolic wave fronts around the defect. As the excitation density is increased, polariton-polariton interactions start to be non-negligible [figure 2 (a-I)], resulting in deviations of the spectrum of excitations from a parabolic shape. At a particular density the linearization of the spectrum of excitations around k_p takes place and a sound

velocity can once more be attributed to the polariton fluid. In contrast to the situation depicted in figure 1, conditions are now such that $v_p > c_s$: the superfluid condition according to the Landau criterion is not satisfied and the defect is able to create linear wave front excitations starting from the defect [figure 2 (a-II)]. At higher densities Čerenkov-like wave fronts can still be distinguished [figure 2 (a-III)]. Figure 2 (b) shows images calculated under similar conditions by solving a Gross-Pitaevskii equation with pumping and decay and a polariton-polariton interaction given by g. More details on the simulated images as well as on the superfluid and supersonic regimes can be found in [19].

4. Polariton superflow in the time-resolved regime.

Key information about the dynamical properties of polariton fluids, such as the relationship between momentum, velocity and dispersion, the diffusion behaviour, and the scattering (or its absence) with defects in different quantum fluid regimes can be accessed by the use of time resolved photoluminescence techniques. However, the extremely short polariton lifetime and the need to *resonantly* create a fluid with an excitation field (a laser beam which would black out the detection of the actual polaritons at the same energy) had prevented so far the follow up of coherent polariton fluids. Recently, a new excitation scheme, the so-called TOPO, based on the Optical Parametric Oscillator (OPO) configuration has allowed the creation and detection of the dynamics of polariton fluids with a well defined momentum and a high temporal resolution [18], circumventing the above mentioned difficulties. Additionally, this configuration allows the exploration of situations in which the phase and coherence of the signal is not fixed by the pump [28,29]. Observations performed with the use of this technique provided the first evidences of superflow of polaritons in semiconductor microcavities via the observation of the unperturbed passage through obstacles of different sizes. Additionally, a clear linearization of the system's dispersion was observed [18]. In this section we will show results on the dynamics of polariton flows created in the TOPO configuration showing some of these facts, providing, along with the results of section 3, a broad picture of polariton phenomena in the quantum fluid regime [4,30].

The sample employed for these experiments is a GaAs/AlGaAs microcavity with a single quantum well placed on the centre of a λ/2 cavity, characterized by a Rabi splitting of 4.4 meV. All experiments have been performed at 10 K with the use of two Titanium:Sapphire lasers as excitation sources: a cw laser and a 2 ps pulsed one. Images of the near and far field of the emission are formed, in reflection geometry, on the entrance slit of a spectrometer attached to a streak camera, enabling the recording of two dimensional space and momentum maps of the luminescence resolved in energy and time, with a temporal resolution of ~5 ps.

The schematics of the TOPO operation are depicted in figure 3 (b). A cw pump excites the microcavity resonantly with the lower polariton branch with momentum k_p, in a spot of about 100 μm in diameter. If its power is high enough, OPO operation will start with signal emission at $k = 0$ [31]. In our case we additionally shine a resonant pulsed laser at an angle resulting in an equivalent polariton momentum k_i, which will act as a seed for the onset of parametric oscillation, resulting in a signal with momentum $k_s = 2k_p - k_i$, which can be finely controlled by the choice of pump and idler angles of incidence. The pulsed idler is focused on a spot of 16 μm within the pump spot. When the idler pulse reaches the sample, a signal polariton packet is formed, which starts to move ($k_s \neq 0$). Once the idler has disappeared the signal packet keeps being replenished by stimulated scattered polaritons coming from the pump field. More details on the TOPO mechanism can be found elsewhere [18,32].

Figure 3 shows real (a) and momentum (c) space images of the spectrally selected signal polariton wave-packet created by the TOPO at different times after the arrival of the pulsed idler. The pump and idler angles of incidence are 10º and 16º, respectively. The signal packet is created with a well defined momentum of 0.60 μm^{-1} [the momentum distribution at 2 ps –not shown- shows the same shape as that at 16 ps, (c-II)], and moves a long a distance of 40 μm, without appreciable alterations of its Gaussian shape. In the course of its trajectory, the polariton packet encounters two deep localized defects,

indicated by black dots in (a-III), which are traversed without noticeable change of its shape both in real and momentum space. Remarkably, the wave vector of the packet is well preserved until the moment when the packet reaches the edge of the excitation spot (a-IV, c-IV), indicating that its coherence is well defined during the whole time of flight. Note that the density wave fronts observed in the polariton fluid when it traverses any of the defects do not arise as a consequence of the direct scattering of signal polaritons with these potential barriers. These fronts reflect the density modulation created on the pump polariton field which is injected at a much higher momentum, when interacting with the same defects. The pump polaritons, moving with a high momentum, are subject to scattering with the defects in a similar way to that depicted in figures 1 (c-I-II), 2 (a-I-II) and 2 (b-I-II) in the upstream direction. The density fluctuations of the pump are reflected on the signal fluid that they feed, when it traverses these regions.

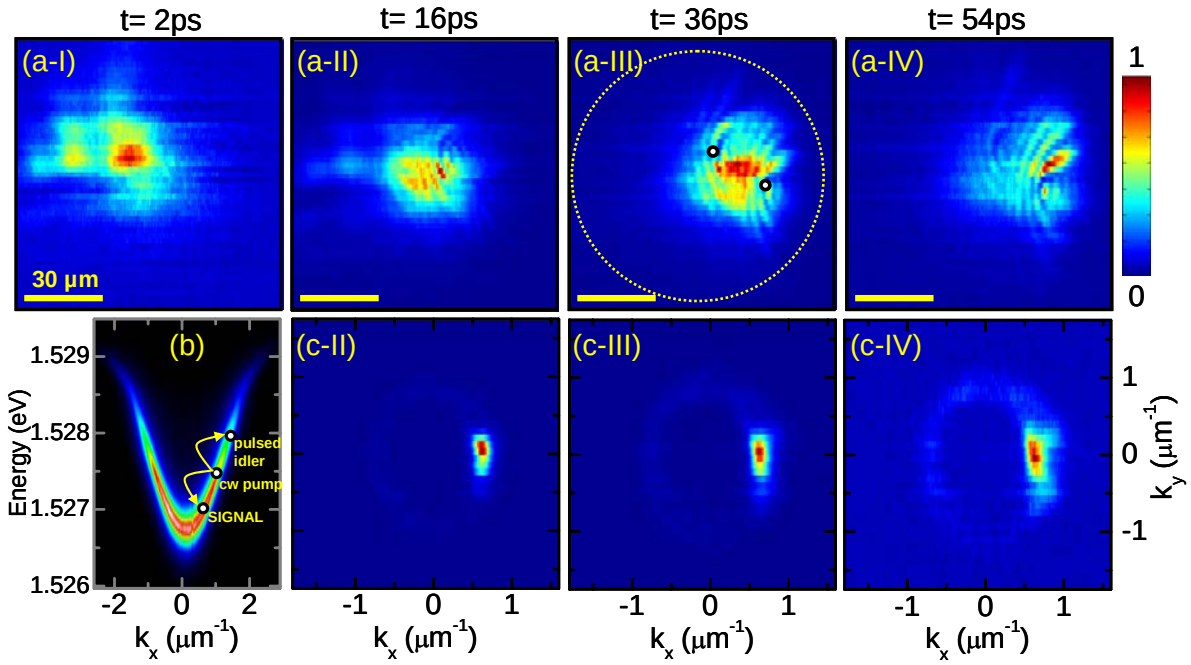

Figure 3. Real (a) and corresponding momentum space (c) images of a polariton fluid created at $t = 0$, after the arrival of the pulsed idler at an angle of incidence of 16º and a pump incidence at 10º. The momentum distribution at $t = 2$ ps (not shown) presents the same features as that at $t = 2$ ps. Black dots in (a-III) indicate the position of two localized defects, while the dotted circle shows the area over which the pump spot extends. Each image has been normalized to its maximum intensity. (b) Lower polariton branch luminescence under non-resonant excitation showing a scheme of the TOPO.

Figures 3 (a) and (c) remarkably show the absence of scattering when the signal polariton fluid encounters a localized potential barrier in its flow-path, evidencing superfluid behaviour in the sense of flow without friction. In the context of the Landau model used to explain the results of section 2, this would correspond to the onset of the inhibition of excitations for the signal packet.

An additional significant characteristic of the signal emission in the TOPO configuration is that it presents a linear dispersion. Figure 4 (a) –upper panel–depicts the observed photoluminescence of the signal, integrated over its whole time of flight, under the conditions of figure 3. The linearization of the emission around the signal (arrow) contrasts with the parabolic one observed under out of resonance excitation (lower panel). A strong blueshift of 0.6 meV between the two situations is also observed. Figure 4 (b) shows the expected emission in energy-momentum space calculated by solving a one-dimensional Gross-Pitaevskii equation with decay including the cw pump and pulsed idler excitation. It is readily observed that both the blueshift and the linearization of the dispersion arise

from the strong polariton-polariton interactions in the macroscopically occupied signal, pump and idler fluids [33].

One of the direct consequences of the signal polaritons moving on top of a linearized section of the dispersion is that the signal polariton wave packet does not spread in space (neither in *k*), as observed in figure 3. All the fluid components remain in phase, with the same speed (given by the slope of the dispersion [32]), preventing the spreading. Simulations of the time evolution of the signal fluid based on the above mentioned one dimensional Gross-Pitaevskii equation in the conditions resulting in the dispersions shown in figure 4 (b), yield packet flows with a well preserved width in real and momentum spaces [18].

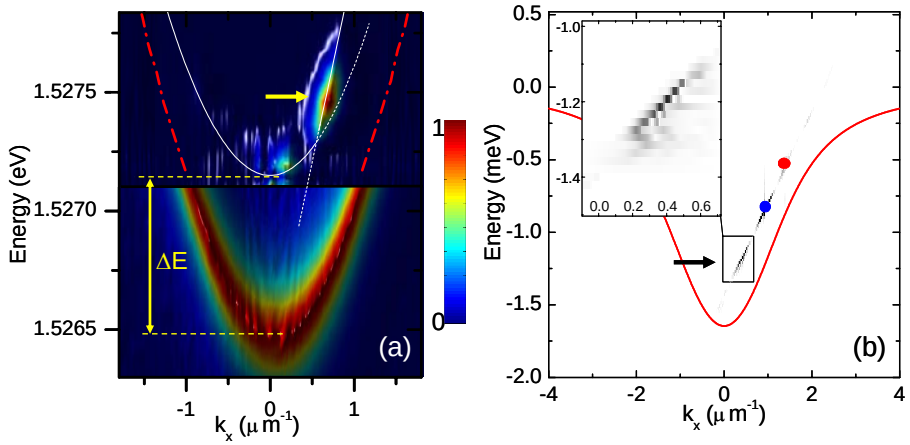

Figure 4. (a) Experimentally observed lower polariton branch dispersion under the TOPO conditions described in figure 2 (upper panel), and under non-resonant excitation (lower panel). ΔE indicates the blueshift induced by polariton-polariton interactions. The yellow arrow indicates the signal state. (b) Calculated dispersion under cw pump (blue dot) and pulsed idler (red dot) illumination. The inset is a zoom-in of the signal states (marked by the black arrow). From [18].

5. Conclusions

We have presented a comprehensive set of experiments in different excitation configurations showing evidences of superfluidity of polaritons in the sense of flow without scattering when traversing an obstacle. Our results under cw resonant excitation can be well described by the Landau model of superfluidity, with the existence of a critical flow velocity for the onset of perturbations in the fluid. In addition to the observation of frictionless motion, the time resolved experiments, open the way to new methods to study the ultrafast dynamics of quantum fluids, with prospective applications on the research of spontaneous [29] and non-spontaneous phase transitions. Additionally, the fine control of the size and initial state of the polariton condensates through the resonant optical excitation, enables the address of other questions like the formation of Josephson oscillations [34] or if the size of the droplet plays a role in the system's spectrum of excitations as it is the case in liquid ^{4}He, for instance [35,36]. This last subject may present interesting particularities in a dissipative system like that conformed by polaritons in which the particle number is not conserved.

Acknowledgements

This work was partially supported by the *Ile de France* programme IFRAF, the *Agence Nationale pour la Recherche* (ANR-07-NANO-GEMINI), the Spanish MEC (MAT2008-01555 and QOIT-CSD2006-00019) and the CAM (S2009/ESP-1503). A.B. is a member of the Institut Universitaire de France.

References

[1] Kapitza P 1938 *Nature (London)* **141** 74
[2] Allen J F and Misener A D 1938 *Nature (London)* **141** 75

[3] Leggett A J 2001 *Rev. Mod. Phys.* **73** 307
[4] Carusotto I *talk at ICSCE 4 conference (Cambridge, UK, 2008), available at* http://www.tcm.phy.cam.ac.uk/BIG/icsce4/talks/carusotto.pdf
[5] Hess G B and Fairbank W M 1967 *Phys. Rev. Lett.* **19** 216
[6] Chevy F, Madison K W and Dalibard J 2000 *Phys. Rev. Lett.* **85** 2223
[7] Vinen W F 1961 *Proc. R. Soc. Lond. A* **260** 218
[8] Whitmore S C and Zimmermann W 1968 *Phys. Rev.* **166** 181
[9] Ryu C, Andersen M F, Clade P, Natarajan V, Helmerson K and Phillips W D 2007 *Phys. Rev. Lett.* **99** 260401
[10] Williams G A and Packard R E 1974 *Phys. Rev. Lett.* **33** 280
[11] Madison K W, Chevy F, Wohlleben W and Dalibard J 2000 *Phys. Rev. Lett.* **84** 806
[12] Landau E M and Lifshitz L D 1986 *Statistical Physics, Parts I and II* (Pergamon Press).
[13] Allum D R, McClintock P V E, Phillips A and Bowley R M 1977 *Phil. Trans. R. Soc. Lond. A* **284** 179
[14] Note that in ^{4}He due to the existence of a roton minimum in the spectrum of excitations, the actual critical velocity is lower than the speed of sound.
[15] Hartmann M, Mielke F, Toennies J P, Vilesov A F and Benedek G 1996 *Phys. Rev. Lett.* **76** 4560
[16] Chikkatur A P, Görlitz A, Stamper-Kurn D M, Inouye S, Gupta S and Ketterle W 2000 *Phys. Rev. Lett.* **85** 483
[17] Raman C, Köhl M, Onofrio R, Durfee D S, Kuklewicz C E, Hadzibabic Z and Ketterle W 1999 *Phys. Rev. Lett.* **83** 2502
[18] Amo A, Sanvitto D, Laussy F P, Ballarini D, Valle E d, Martin M D, Lemaitre A, Bloch J, Krizhanovskii D N, Skolnick M S, Tejedor C and Viña L 2009 *Nature* **457** 291
[19] Amo A, Lefrère J, Pigeon S, Adrados C, Ciuti C, Carusotto I, Houdré R, Giacobino E and Bramati A 2009 *Nature Phys.* **5** 805
[20] Kasprzak J, Richard M, Kundermann S, Baas A, Jeambrun P, Keeling J M J, Marchetti F M, Szymanska M H, Andre R, Staehli J L, Savona V, Littlewood P B, Deveaud B and Dang L S 2006 *Nature* **443** 409
[21] Balili R, Hartwell V, Snoke D, Pfeiffer L and West K 2007 *Science* **316** 1007
[22] Lai C W, Kim N Y, Utsunomiya S, Roumpos G, Deng H, Fraser M D, Byrnes T, Recher P, Kumada N, Fujisawa T and Yamamoto Y 2007 *Nature* **450** 529
[23] Lagoudakis K G, Wouters M, Richard M, Baas A, Carusotto I, Andre R, Dang L S and Deveaud-Pledran B 2008 *Nature Physics* **4** 706
[24] Sanvitto D, Marchetti F M, Szymanska M H, Tosi G, Baudisch M, Laussy F P, Krizhanovskii D N, Skolnick M S, Marrucci L, Lemaitre A, Bloch J, Tejedor C and Viña L 2009 *arXiv:0907.2371v2*
[25] Carusotto I and Ciuti C 2004 *Phys. Rev. Lett.* **93** 166401
[26] Ciuti C and Carusotto I 2005 *Phys. Stat. Sol. (b)* **242** 2224
[27] Carusotto I, Hu S X, Collins L A and Smerzi A 2006 *Phys. Rev. Lett.* **97** 260403
[28] Krizhanovskii D N, Sanvitto D, Love A P D, Skolnick M S, Whittaker D M and Roberts J S 2006 *Phys. Rev. Lett.* **97** 097402
[29] Ballarini D, Sanvitto D, Amo A, Viña L, Wouters M, Carusotto I, Lemaître A and Bloch J 2009 *Phys. Rev. Lett.* **102** 056402
[30] Keeling J and Berloff N G 2009 *Nature* **457** 273
[31] Whittaker D M 2005 *Phys. Rev. B* **71** 115301
[32] Amo A, Sanvitto D and Viña L *Semic. Science and Technol. (accepted)*
[33] Wouters M and Carusotto I 2007 *Phys. Rev. A* **76** 043807
[34] Sarchi D, Carusotto I, Wouters M and Savona V 2008 *Phys. Rev. B* **77** 125324
[35] Sindzingre P, Klein M L and Ceperley D M 1989 *Phys. Rev. Lett.* **63** 1601
[36] Krishna M V R and Whaley K B 1990 *J. Chem. Phys.* **93** 746